PISTON ERROR EFFECT ON INTENSITY AT THE INTERACTION OF COHERENTLY COMBINED FEMTOSECOND LASER BEAMS WITH CONE TARGETS

Laura IONEL[1]

Coherent beam combination is an actual powerful tool for extreme fields generation through the superposition of multiple coherent laser beams in specific conditions. Implementing such a tool in laser-matter interaction experiments makes it possible to generate output intensities of the laser beams up to 10^{23} W/cm^2 and beyond in accordance to the current scientific requirements. In this context, we developed a numerical study of the laser intensity dynamics at the interaction of coherently superimposed beams with conical targets under the piston error effect. The evolution of the laser field dynamics is numerically investigated in the laser - matter interaction area for four different materials of the micro-patterned conical targets. This theoretical simulation analysis demonstrates that a controllable laser intensity improvement with sub-wavelength resolution in a two - superimposed beams configuration can be achieved by introducing a temporal displacement between the two coherent sources. These results are of great interest for various experiments which employ the superposition of two or more coherent laser beams in laser matter interaction schemes for laser intensity enrichment.

Keywords: Coherent beam combination, ultra-short laser pulses, ultrafast laser–micro-patterned conical target interaction, pulse shaping.

1. Introduction

In the last decades, the ultra-fast and ultra-intense laser systems have registered remarkable progresses in fundamental and applied research [1-6] being successfully implemented in a wide range of applications due to their high emitted power, short pulse duration and the advantage of the micro-processing precision from life science to nuclear and high-energy density physics [7-12]. In the frame of the actual scientific requirements in terms of high intensities beyond 10^{23} W/cm^2, a promising tool which may facilitate the generation of such extreme intensities is represented by the coherent beam combination (CBC) technique. This method represents an optimum solution of power scaling by combining coherent beams while maintaining the beam quality and a lower losses level [13-15]. This versatile technique exhibited significant progresses in the last decade, being employed in a broad range of scientific applications such as: laser beam spatial modulation [16], self-imaging combiners [17], space science [18], industrial processing [19], fibre

[1] Researcher, National Institute for Laser, Plasma and Radiation Physics, Romania, e-mail: laura.ionel@inflpr.ro

accelerators [20], gravitational wave detection [21], diffractive optics [22] or nuclear physics [23]. For a high-efficient laser field enrichment in the focal point, the CBC method requires a high-quality beams profile and an accurate control on the compound laser field intensity dynamics.

Beside this, the superposition of the coherent laser beams exhibits progressive distortions of the compound beam induced by the piston fluctuations or tilt error which significantly influence the CBC method performance. Recent studies related to the active and passive phase control of the progressive distortions using an optical principle as self-phase locking [24-27] or CBC optimization using deep learning [28, 29] could bring significant contribution to the coherently beams superposition efficiency.

Considering the previous numerical approaches concerning the coherent beams superposition employing ultra-short and ultra-intense pulsed lasers [30-32], in the present work we numerically investigated the laser intensity dynamics in coherently overlapped laser beams – micro-patterned conical target interaction system under the piston error effect introduced by moving one of the laser sources in the propagation direction while the second one remains fixed. Thus, the laser source shift induces a temporal displacement between the two coherent laser sources with subwavelength resolution according to the equivalent relation $s=c\cdot t$, where s denotes the spatial extension of the laser pulse, c represents the velocity of light being equal to $3\cdot10^8$ m/s and t is the duration of the laser pulse [33, 34]. The present high-power laser experiments which imply CBC technique require a precise control of piston error effect in order to mitigate significant distortions of the resulted laser beam which may occur and further lead to intensity reduction. Considering these, the aim of this approach is to provide a purposive solution to the actual demands in terms of adjustable laser field increase maintaining an excellent beam quality during the coherent laser beams overlapping (CLBO) process starting from previously discussed laser-conical target interaction scenarios [35-39]. The intensity analysis is performed by using a numerical approach based on finite-difference time domain (FDTD) computations which offers a broad description of the compound EM field distribution in the focal area. The numerical results have been disclosed taking into account the spatio-temporal aspects of focused ultra-short laser pulses distribution providing an essential contribution to the scientific field of intense pulsed lasers which could be broadly used for various high-intensity laser solid target interaction experiments.

2. Numerical models

The coherently overlapping of ultra-short laser beam and piston error effect were investigated by using a two-dimensional numerical model based on FDTD approach. This method is an explicit solution to Maxwell's curl equations being

widely used as a propagation solution approach in large-scale integrated quantum optics with no approximations or theoretical restrictions. Here, Maxwell's equations synthesize the dependence between the temporal change in the electric field and the spatial variation of the magnetic field. The 2D numerical model has been performed using the commercial software RSoft [40] which is able to provide scalable scenarios for a wide variety of laser systems configurations. In our approach, the numerical model considered a region of space with no flowing currents or isolated charges. Two of the Maxwell's curl equations to be solved expressed in Cartesian coordinates are:

$$\frac{\partial E_x}{\partial t} = -\frac{1}{\varepsilon}\left(\frac{\partial H_y}{\partial z} - \frac{\partial H_z}{\partial y}\right) \tag{1}$$

$$\frac{\partial H_y}{\partial t} = -\frac{1}{\mu}\left(\frac{\partial E_x}{\partial z} - \frac{\partial E_z}{\partial x}\right) \tag{2}$$

where μ represents the permeability parameter and ε is the permittivity parameter. The other four equations are symmetric equivalents and they are generated by cyclically substituting the x, y and z subscripts and derivates. The situation described by the Maxwell's equations reveals that the change in the electric field E is dependent upon the spatial variation of the magnetic field H, and conversely. According to the FDTD method, the Maxwell's equations are solved by first discretizing the equations via central differences in space and time. The most common method used to solve these equations is based on Yee's mesh [41] being able to calculate the E and H fields components at specific points on a grid. Also, the FDTD numerical model enforces the Courant condition which states that the time step should be correspondingly set to offer enough time to the information to propagate through the space discretization:

$$c\Delta t < \frac{1}{\sqrt{1/\Delta x^2 + 1/\Delta y^2 + 1/\Delta z^2}} \tag{3}$$

where c is the speed of light and Δx, Δy, Δz the grid sizes in all three spatial dimensions of the simulation cell.

The present numerical approach has carefully considered the boundary conditions at the spatial edges of the computational domain based on the perfectly matched layer (PML) simulations [42], which use an absorbing layer, specially designed to absorb the energy without reflection. In our numerical computations, the PML dimension was equal to 0.5 μm on both axes.

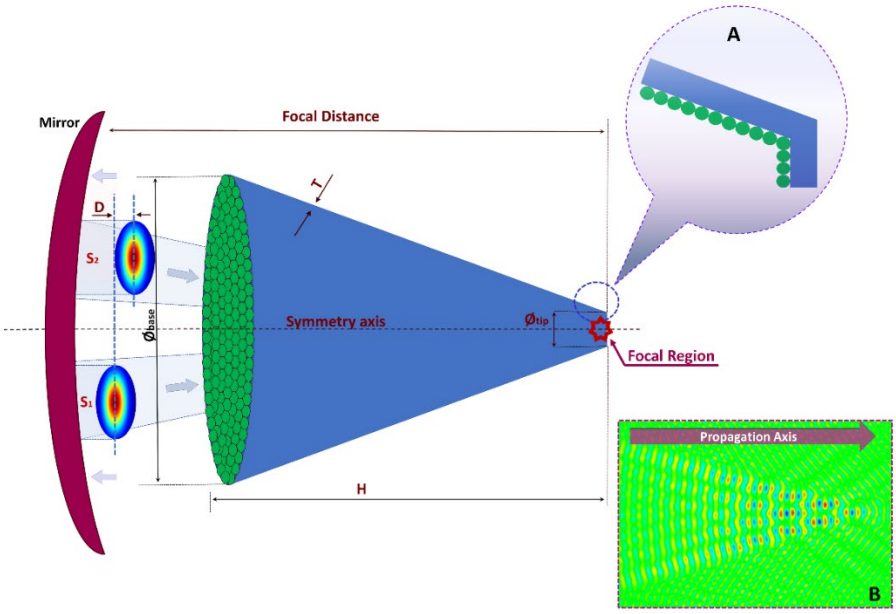

Fig. 1. Graphical design of the optical setup of coherently combined laser beams interaction with a top-flat conical target having a one-layer micro-spheres based internal wall profile (Inset A) in the presence of temporal displacement (D) between the two Gaussian laser sources S1 and S2. Inset B – Spatial distribution of the compound EM field for aluminium material at 25 fs pulse duration.

The schematic illustration of the setup for coherently overlapped laser beams–micro-patterned target interaction is depicted in figure 1. The study considers two identical Gaussian laser sources denoted by S_1 and S_2 both having the diameter of 20 μm, central wavelength of 0.8 μm, pulse duration of 25 fs, symmetrical position relative to the propagation axis (z) and equal output energy values as initial conditions. The value of the angle between the propagation direction and the horizontal axis was chosen to be equal to 30° in accordance to our previous work [32] in terms of laser intensification. The linear s-polarized beams are focused by a parabolic mirror which has the diameter of 150 μm and the focal distance of 120 μm. The piston error effect is produced by inducing a temporal displacement (D) between the two coherent sources in the range of 0-24 μm with variable step. The temporal excitation consists of a sinusoidal carrier waveform multiplied by a Gaussian envelope function which can be defined as:

$$f(t) = exp\left[-\left(\frac{t}{\tau} - t_d\right)^2\right] sin\left[\frac{2\pi}{\lambda}(t) + At^2 + \phi_0\right] \quad (4)$$

where λ represents the central wavelength set to be equal to 800 nm, τ is the pulse duration dependent on the wave cycles number and t_d indicates the delay time dependent on τ. The chirp coefficient of the laser pulse is denoted by A and it is

defined in units of μm^{-2}. The phase ϕ_0 is properly adjusted to be equal to zero when the Gaussian function reaches its maximum value.

The FDTD numerical model could provide a full description of the laser field intensity dynamics in the proximity of the coherent combined beams micro-patterned targets interaction point under the phase and displacement error effect. The sketch of coherently superimposed laser beams–conical targets interaction system illustrated in figure 1, includes beside the incident laser sources, a conical cone target with the height (H) of 80 μm, the large base diameter ϕ_{Base} of 70 μm, the small base diameter ϕ_{Tip} of 10 μm and the thickness of the wall (T) of 4 μm. The length of the computational domain is equal to 200 μm while the width is 170 μm. The background refractive index is equal to 1, the grid size is 0.04 μm and the FDTD method time step value is equal to 0.028 μm. We considered for this study the conical target having a one-layer micro-spheres based internal wall profile with four different materials: Copper, PMMA, Aluminium and Silicon (Table 1) both for the target and the internal microspheres accordingly chosen with the initial investigations performed for this approach. The internal wall profile of the conical target has been chosen in accordance to previous works due to the micro-spheres properties which behave as an array of near-field lenses [43] focusing the incident beam in multiple spots, thereby inducing a local laser field enrichment during the propagation through the target. Thus, by considering a CBC scenario in a conical target with one-layer micro-spheres internal wall profile, a significant laser intensity-improvement in the focal region is expected. The intensity analysis made for the particular case of coherent superposition of two laser sources under the piston error has considered the variation of the dimension of the internal wall microspheres in the range of 1-4 μm with 1 μm step. Considering these variable parameters, we first elaborated a study regarding the electromagnetic field structure in the proximity of coherently superimposed laser beams–micro-patterned conical target interaction point both from spatial and temporal considerations at particular moments of time when the temporal monitors point out the highest laser fields. The temporal monitors are placed in a well-defined configuration in the compound electromagnetic pulse - conical target interaction region being able to deliver the combined beams intensity values under the piston error effect. Numerical and experimental characterization of local mechanisms and physical properties of the material surfaces employing laser sources proves to be an essential tool to provide an extensive characterization of the structures features based on complex quantitative information [44, 45].

The present numerical approach has the aim to describe the spatio-temporal characteristics of the composed EM pulse distribution computed in the proximity of the interaction of the coherently overlapped laser beams with the micro-patterned conical target tip and to point out the influence of the material and target features on the laser field intensity increase in predefined conditions.

Table 1.

Optical parameters of the materials used in the CLBO study

Material	Absorption coefficient (cm^{-1})	Complex refractive index n+ik	
		n	k
Copper	$7.8745 \cdot 10^5$	0.2535	5.0131
PMMA	0.042097	1.4848	-
Aluminium	$1.3123 \cdot 10^6$	2.7673	8.3543
Silicon	1027.9	3.6941	0.0065

3. Results and discussions

The intensity dynamics of the coherently superimposed laser beams has been numerically investigated under the piston error effect in the composed EM pulse micro-patterned conical target interaction area in order to obtain the proper numerical fundaments for an accurate control on laser field intensity in specific conditions. The numerical analysis of the compound laser pulse intensity evolution has been preceded by a particular study on the micro-spheres material and diameter to determine the most efficient ones in terms of laser field enrichment in the interest region. Thus, on the basis of our coherently overlapped laser beams target interaction sketch illustrated in figure 1, we determined the influence of the micro-spheres material and diameter value on the intensity of the composed EM field in the laser target interaction point in focal region for all four materials considered. To investigate the dynamics of the compound laser pulse intensity, the numerical model uses the highest laser field values registered by the time monitors uniformly positioned in the laser target interaction zone. As depicted in figure 2, the highest intensity values are obtained for aluminium micro-spheres of 2 μm diameter. By comparing all four cases, one can observe that highest intensity values were registered for micro-spheres diameter value equal to 2 μm for all four materials considered. Thus, this initial study proved to be essential to determinate the optimum micro-spheres diameter value to be considered for further studies disclosed in this work.

In the frame of the compound EM field distribution analysis, the time monitors are also able to deliver specific data concerning the phase of the longitudinal electric field component E_x. As illustrated in figure 3, the numerical computations of the phase have been performed along the x-axis based on the discrete Fourier transform frequency analysis. In the present study, the phase profile of the composed EM pulse with less variation along the x-axis is obtained for the material with the highest absorption coefficient (aluminium) which is in the agreement with the intensity results previously discussed.

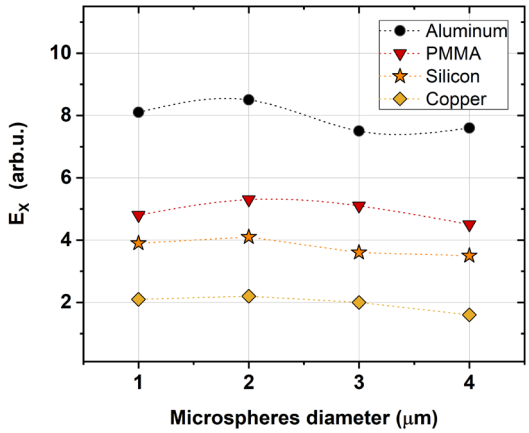

Fig. 2. The micro-spheres material and diameter influence on the intensity of the composed EM field in the proximity of the laser conical target interaction point.

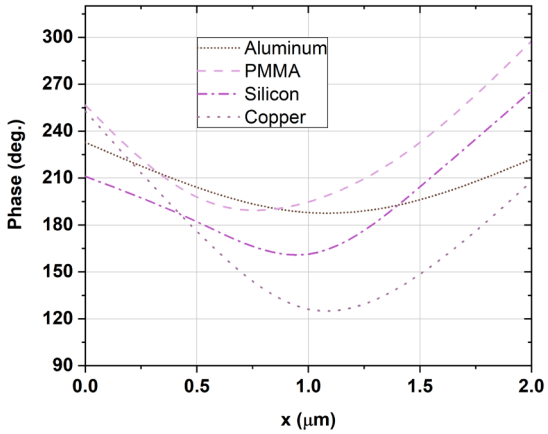

Fig. 3. Lineouts of the phase profile of the compound EM pulse in the interaction area with a micro-patterned cone target considering four distinct materials.

Meanwhile, an advanced study of the laser field intensity dynamics in the proximity of the compound laser beam cone target interaction point has been performed under the piston error effect. As shown in figure 1, the internal target wall presents a one-layer micro-spheres profile, considering the optimum diameter value for each micro-sphere to be equal to 2 μm, as previously specified. Taking into account the focusing properties of each micro-sphere, we investigated the behaviour of the composed EM field structure during the propagation through the target both from spatial and temporal point of view. First, we analysed the electromagnetic field distribution from spatial point of view in different points in the proximity of the coherently overlapped laser beam conical target interaction zone in the presence of temporal displacement between the two laser sources along the propagation direction in the range of 0-24 μm with a variable step. The insets

of figure 4 depict the case of spatial extension of the compound EM field for three distinct values of piston error (D=0 μm, 0.4 μm and 0.8 μm) for aluminium material at 25 fs pulse duration.

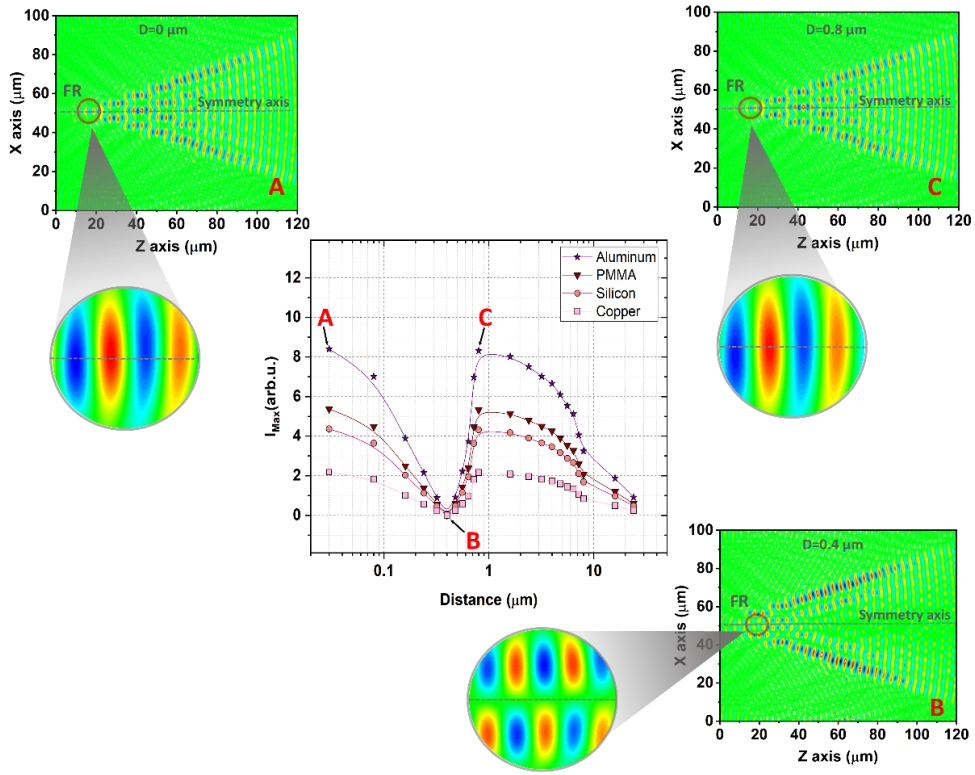

Fig. 4. The evolution of the intensity laser field measured by the time monitors uniformly positioned in the coherently superimposed beams cone target interaction zone under the piston error effect for all four materials considered. Insets: the laser field distribution in the focal region (FR) for different temporal displacement values (A) D=0 μm, (B) D=0.4 μm, (C) D=0.8 μm for aluminium material.

A complex investigation of the composed EM pulse evolution in the proximity of the laser target interaction point had been performed by computing the corresponding value of the laser intensity for all four materials considered in the present study under the piston error effect. Thus, for a temporal displacement value equal to 0.4 μm, the field intensity in the laser target interaction point is close to zero while the field distribution is divided in two symmetrical lobes comparing to the other two resulted spatial distributions of the laser field computed for the cases of D equal to 0 and 0.8 μm respectively, which register the highest values of the laser intensity.

As a first remark, the numerical results presented in figure 4 reveal that the EM field exhibits a similar behaviour as function of piston error for all four investigated

cases. Moreover, it can be noticed that the maximum intensity value is obtained for the case of aluminium material being a factor of almost 4 larger than the one obtained for the case of cooper material under the piston error effect in the range of 0 – 0.8 μm, except for the case of D=0.4 μm when the laser field is close to zero for all four materials.

As expected, by considering a flat-top conical target with one-layer micro-spheres based internal wall profile we could obtained a noticeable field intensity increase which is of great interest in a wide area of actual ultra-short pulse laser applications. As a general remark, it is noticeable that the material refractive index and the micro-patterned profile of the internal wall of the conical target impose an essential contribution to the laser field intensification in well-defined conditions. Moreover, it has been shown that this effect depends on the structure of the laser field and either on the geometric features of the laser target interaction setup demonstrating that the laser field intensity can be precisely adjusted with sub-wavelength resolution in case of coherently superimposed laser beams.

The temporal aspects of the compound EM field distribution under the piston error effect have been investigated by implementing the spatio-temporal correlation in the proximity of the laser conical target interaction point, determining the temporal FWHM values for each case. In order to represent the evolution of the temporal extension of the EM field, the temporal data given by the time monitors is converted in spatial one using the Minkowski space relation $s=c\cdot t$, as described in our previous works [36,37]. The numerical computations are performed along the propagation axis in units of $c\cdot t$ considering that 10 μm corresponds to 33,3 fs. The temporal study uses similar conditions previously considered in the intensity dynamics analysis.

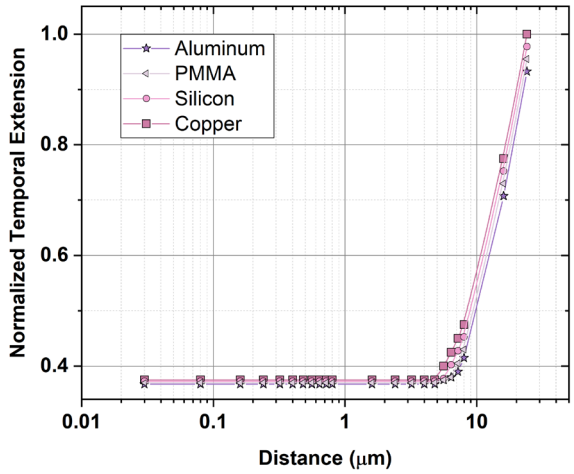

Fig. 5. Normalized temporal extension of the composed EM pulse in the laser cone target interaction point for all four materials considered for phase error values comprised in the range λ/10 and 30λ. The maximum reduction of temporal duration of the combined pulse has been registered in case of aluminium for all piston error values.

It is important to note that the temporal FWHM changes, determined for each piston error value, correspond to the spectral broadening of the composed EM pulse in the laser target interaction point. This aspect is a consequence of the Fourier relation between the spectral distribution and the temporal evolution of the pulse. One can observe in figure 5 a similar behaviour of the temporal FWHM values of the compound EM field for all four materials considered under the piston error effect. Thus, as a general overview of the normalized temporal extension study, the FWHM of the temporal extension of the composed laser pulse exhibits a constant behaviour for phase error values comprised in the range $\lambda/10$ and 10λ while for piston error values higher than 10λ a considerable increase of the temporal extension has been registered. These aspects could be taken into account in the high-power laser experiments which employ CLBO method for an accurate intensity control.

As an overall result, the numerical computations reveal that the piston error effect induces a maximum reduction of temporal duration of the combined pulse in case of aluminium for all temporal displacement values. This numerical approach was exclusively focused on the spatio-temporal aspects of electromagnetic field distribution in the laser target interaction area under the piston error effect. Additional numerical studies concerning the plasma motion in ultra-intense laser fields, the morphology, specific parameters of the materials and particular effects which have contributed to the spatial modulation of the electromagnetic field that leads to the increase of the composed EM pulse intensity in the interaction area, are envisaged to be individually investigated in a future work.

4. Conclusions

The obtained results show that, in the context of coherently superimposed beams scenario, the geometry and the materials of the targets influence significantly the evolution of the compound laser field intensity in the proximity of the laser matter interaction point, under the piston error effect offering a complex characterization of the field enrichment process obtained in predefined conditions. The highest intensity values and the maximum reduction of temporal duration of the combined pulse has been registered in case of aluminium for all piston error values. Taking into consideration the overview of the electromagnetic field distribution modelled with the FDTD computations, our study demonstrates that the laser field intensity can be precisely controlled with sub-wavelength resolution in case of coherently superimposed laser beams by inducing a temporal displacement between the two coherent laser sources improving in this way the beam quality which represent a major quest of the coherent beams overlapping. This method can be used as a highly accurate technique to adjust the laser intensity increase in various ultra-short and ultra intense laser applications.

Acknowledgements

– The research is supported by the Romanian Ministry of Research, Innovation and Digitalization under Romanian National Nucleu Program LAPLAS VII – contract no. 30N/2023, PN-III-P4-IDPCE2021-8 and PN-III-P1-1.1-TE2021-1546.

R E F E R E N C E S

[1] *G. A. Mourou, N. J. Fisch, V. M. Malkin, Z. Toroker, E. A. Khazanov, A. M. Sergeev, T. Tajima, B. Le Garrec,* Exawatt-Zettawatt pulse generation and applications, Opt. Commun. **285** 2012, 720–4

[2] *F. Lureau, et al.,* High-energy hybrid femtosecond laser system demonstrating 2 × 10 PW capability, High Power Laser Sci. Eng. **8** 2020, 15

[3] *O. Budriga, C. M. Ticos,* Modeling the electron acceleration in relativistic channels for space irradiation applications, Plasmas Phys. Control. Fusion **62** 2020, 124001

[4] *K. Fleck, N. Cavanagh, G. Sarri,* Conceptual design of a high-flux multi-GeV gamma-ray spectrometer, Sci. Rep. **10** 2020, 9894

[5] *X-L Zhu, T-P Yu, Z-M Sheng, Y. Yin, I. C. E. Turcu, A. Pukhov,* Dense GeV electron–positron pairs generated by lasers in near-critical-density plasmas, Nature Commun. **7** 2016, 13686

[6] *A. H. Zewail*, Femtochemistry. Past, present, and future, Pure Appl. Chem **72** 2000, 2219–2231

[7] *Y. Arikawa, Y. Kato, Y. Abe, S. Matsubara, H. Kishimoto, N. Nakajima, A. Morace, A. Yogo, H. Nishimura, M. Nakai, S. Fujioka, H. Azechi, K. Mima, S. Inoue, Y. Nakamiya, K. Teramoto, M. Hashida, S. Sakabe*, Effective and repetitive neutron generation by double-laser-pulse driven photonuclear reaction, Plas. Fus. Res. **13** 2018, 2404009

[8] *S. S. Bulanov*, Accelerating protons to therapeutic energies with ultraintense, ultraclean, and ultrashort laser pulses, Med. Phys. **35**(5) 2008, 1770–1776

[9] *F. Negoita, et al.,* Laser driven nuclear physics at ELI-NP, Rom. Rep. Phys. **68** 2016, S37–144

[10] *I. C. E. Turcu, et al*., High field physics and QED experiments at ELI-NP, Rom. Rep. Phys. **68** 2016, S145–231

[11] *D. Ursescu, et al.,* Laser beam delivery at ELI-NP, Rom. Rep. Phys. **68** 2016, S11–36

[12] *P. Boller, et al.,* First on-line detection of radioactive fission isotopes produced by laser-accelerated protons, Sci. Rep. **10** 2020, 17183

[13] W. Liang, N. Satyan, F. Aflatouni, A. Yariv, A Kewitsch, G. Rakuljic, H. Hashemi, Coherent beam combining with multilevel optical phase-locked loops, J. Opt. Soc. Am. B 24 (12) 2930-2939 (2007)

[14] Andrusyak, O., Smirnov, V., Venus, G., Glebov, L., "Beam combining of lasers with high spectral density using volume Bragg gratings", Optics Communications, 282(13), 2560-2563 (2009)

[15] A. Klenke, E. Seise, J. Limpert, A. Tünnermann, Basic considerations on coherent combining of ultrashort laser pulses, Opt. Exp. 19(25) 25379 (2011)

[16] *M. Veinhard, S. Bellanger, L. Daniault, I. Fsaifes, J. Bourderionnet, C. Larat, E. Lallier, A. Brignon, J-C Chanteloup*, Orbital angular momentum beams generation from 61 channels coherent beam combining femtosecond digital laser, Opt. Lett. **46**(1) 2021, 25-28

[17] *Y. Liu, Y. Li, Y. Yan, Y. Li, S. Huang, W. Wu, H. Lin, J. Wang, R. Tao,* Self-imaging-based high-power all-fiber coherent combiners: fabrication and preliminary demonstration, Opt. Lett. **48**(6) 2023, 1538-1541

[18] *R. Soulard, M. N. Quinn, T. Tajima, G. Mourou*, ICAN: a novel laser architecture for space debris removal Acta Astronaut **105** 2014, 192-200

[19] *E. Shekel, Y. Vidne, B. Urbach,* 16 kW single mode CW laser with dynamic beam for material processing, Proc. SPIE **11260** 2020, 1126021

[20] *G. Mourou, B. Brocklesby, T. Tajima, J. Limpert*, The future is fibre accelerators, Nat. Photon. **7** 2013, 258-61

[21] F. Wellmann, N. Bode, P. Wessels, L. Overmeyer, J. Neumann, B. Willke, D. Kracht, Low noise 400 W coherently combined single frequency laser beam for next generation gravitational wave detectors, Optics Express 29(7) 2021, 10140-10149

[22] *E. I. Scarlat, M. Mihăilescu, A. Sobetkii*, Spatial frequency and fractal complexity in single-to-triple beam holograms, Journ. Optoel. Adv. Mat. **12**(1) 2010, 105-109

[23] *C. N. Danson, et al*., Petawatt and exawatt class lasers worldwide, High Power Laser SciEng **7** 2019, e54
[24] *S. M. Redmond, K. J. Creedon, J. E. Kansky, S. J. Augst, L. J. Missaggia, M. K. Connors, R. K. Huang, B. Chann, T. Y. Fan, G. W. Turner, A. Sanchez-Rubio,* Active coherent beam combining of diode lasers, Opt. Lett. **36**(6) 2011, 999-1001
[25] *Y. Xue, B. He, J. Zhou, Z. Li, Y. Fan, Y. Qi, C. Liu, Z. Yuan, H. Zhang, Q. Lou,* High power passive phase locking of four yb-doped fiber amplifiers by an all-optical feedback loop, Chin. Phys. Lett. **28**(5) 2011, 054212
[26] *M. Fridman, M. Nixon, N. Davidson, A. A. Friesem,* Passive phase locking of 25 fiber lasers, Opt. Lett. **35**(9) 2010, 1434-1436
[27] Q. Chang, T. Hou, H. Chang, P. Ma, R. Su, Y. Ma, P. Zhou, Iteration-free, simultaneous correction of piston and tilt distortions in large-scale coherent beam combination systems, Optics Express , 29(21) 2021, 34863
[28] *B. Mills, J. A. Grant-Jacob, M. Praeger, R. W. Eason, J. Nilsson, M. N. Zervas*, Single step phase optimization for coherent beam combination using deep learning, Sci Rep. **12** 2022, 5188
[29] *H. Tünnermann, A. Shirakawa*, Deep reinforcement learning for coherent beam combining applications, Opt. Exp. **27**(17) 2019, 24223-24230
[30] *L. Ionel, D. Ursescu*, Non-collinear spectral coherent combination of ultrashort laser pulses, Opt. Express **24** 2016, 704654
[31] *D. Ursescu, L. Ionel*, Spatial and temporal dynamics of ultra-short pulses coherent beam combining, Proc. of SPIE **7501** 2009, 750103
[32] *L. Ionel*, Spatio-temporal analysis of non-collinear femtosecond pulses combination, U.P.B. Sci. Bull., Series A **81**(3) 2019, 271-278
[33] J. W. Yoon, J. S. Shin, D. H. Beak, H. J. Kong, "Piston error characteristics of the self- phase-controlled stimulated Brillouin scattering phase conjugate mirrors", Optics Communications 282, 1000-1003 (2009)
[34] D. Ursescu, L. Ionel, Spatial and temporal dynamics of ultra-short pulses coherent beam combining, Proc. of SPIE 7501 2009, 750103
[35] *L. Ionel*, Characterizing spatio-temporal aspects of chirped pulse amplification laser micro-cone target interaction, Laser Phys. **32** 2022, 035301
[36] *L. Ionel*, Spatio-temporal analysis of high-power laser micro-structured targets interaction, Phys. Scr. **95** 2020, 105501
[37] *L. Ionel*, Numerical analysis of non-collinear coherently combined laser beams interaction with micro-structured targets, Opt. Commun. **498** 2021, 127234
[38] *O. Budriga, E. d'Humieres, L. Ionel, M. Budriga, M. Carabas*, Modelling the interaction of an ultra-high intensity laser pulse with nano-layered flat-top cone targets for ion acceleration, Plasma Phys. Controlled Fusion **61** 2019, 085007:1–15
[39] *O. Budriga, L. Ionel, D. Tatomirescu, K. A. Tanaka,* Enhancement of laserfocused intensity greater than 10 times through a re-entrant cone in the petawatt regime, Opt. Lett. **45** 2020, 3454-3457
[40] https://optics.synopsys.com/rsoft/
[41] K. S. Yee, Numerical solution of initial boundary value problems involving Maxwell's equations in isotropic media, IEEE Trans. Antennas Propagat., AP-**14** 1966, 302
[42] J. P. Berengers, A Perfectly Matched Layer for the Absorption of Electromagnetic Waves, J. Comput. Phys., **114** 1994, 185
[43] *S. Kwon, J. Park, K. Kim, Y. Cho, M. Lee*, Microsphere-assisted, nanospot, non-destructive metrology for semiconductor devices, Light: Science & Applications **11** 2022, 32
[44] *M. Mihailescu, I. A. Paun, M. Zamfirescu, C. R. Luculescu, A. M. Acasandrei, M. Dinescu*, Laser-assisted fabrication and non-invasive imaging of 3D cell-seeding constructs for bone tissue engineering, Journal of Materials Science, **51** 2016, 4262–4273
[45] *M. Stafe, G. C. Vasile, C. Neguţu, A. A. Popescu, L. Baschir, M. Mihăilescu, N. N. Puşcaş*, Analysis of the optical absorption and photoinduced birefringence in As_2S_3 chalcogenide films, U.P.B. Sci. Bull., Series A, **78**(1) 2016, 243-256